The effect of electron-ion collisionality on ETG turbulence

G. J. Colyer,[1,2] A. A. Schekochihin,[2] C. M. Roach,[1] M. A. Barnes,[2,1,3] Y.-c. Ghim,[2,1,*] W. Dorland,[4,2] and F. I. Parra[2,1]

[1] *CCFE, Culham Science Centre, Abingdon, Oxon, OX14 3DB, UK*
[2] *Rudolf Peierls Centre for Theoretical Physics, 1 Keble Road, Oxford, OX1 3NP, UK*
[3] *Plasma Science & Fusion Center, 167 Albany Street, Cambridge, MA 02139, USA*
[4] *University of Maryland, College Park, MD 20742-4111, USA*

In electrostatic simulations of MAST plasma at electron-gyroradius scales, using the local flux-tube gyrokinetic code GS2 with adiabatic ions, we find that the long-time saturated electron heat flux (the level most relevant to energy transport) decreases as the electron collisionality decreases. At early simulation times the heat flux quasi-saturates at a level independent of electron collisionality; however the zonal fluctuation component continues to grow slowly until much later times, eventually reducing the heat flux at low collisionality. We outline an explanation of this effect based on zonal-nonzonal interactions and the scaling of the zonal damping rate with electron-ion collisionality.

Improved energy confinement with decreasing collisionality has previously been observed on NSTX and MAST, and is favourable towards the performance of future devices.

INTRODUCTION

In STs there is experimental evidence for the dependence of energy transport on collisionality [1, 2]. In MAST, Valovič et al. found that the energy confinement time $\tau_E \sim \nu_{*e}^{-0.8\pm0.1}$ [2]. Such a scaling is favorable towards improved confinement in future, hotter devices. There is also experimental evidence that NBI-heated MAST plasmas have high levels of sheared toroidal flow in which anomalous ion transport can be substantially suppressed [3]. Previous gyrokinetic simulations [4] support the paradigm that flow shear can stabilize otherwise unstable linear modes at ion gyroradius scales. Turbulence driven at electron gyroradius scales, in particular by the electron temperature gradient (ETG), may therefore govern confinement.

In this paper, we study the dependence of the electron heat flux Q_e on the electron collisionality ν_e in a simple paradigm: with gyrokinetic electrons and hydrogenic adiabatic ions (AI) in the electrostatic limit ($\delta\mathbf{B} = 0$). We will argue that $Q_e \propto \nu_{ei}$, the electron-ion collisionality, close to experimental values of R/L_{T_e}, and that this scaling is associated with the collisional damping of zonal flows. We will show that at low ν_{ei}, the slow evolution of the nonlinear turbulent state means that simulations of ETG turbulence must run to long times to reach saturation.

NUMERICAL SET-UP

We use the GS2 code [5] to solve for the perturbed electron distribution function $g = \langle \delta f \rangle = e\langle\phi\rangle F/T + h$, where e is the electron charge, ϕ the perturbed electrostatic potential, T the electron temperature, F the background Maxwellian, $\langle\cdot\rangle$ denotes the gyroaveraging operator (here at constant gyrocentre coordinate), and h satisfies the electrostatic gyrokinetic equation (GKE)

$$\frac{\partial h}{\partial t} + \left(v_\parallel \mathbf{b} + \mathbf{v}_d\right)\cdot\nabla h + \langle \mathbf{v}_E\rangle\cdot(\nabla h + \nabla F) = \langle C[h]\rangle - \frac{e}{T}\frac{\partial\langle\phi\rangle}{\partial t}F. \qquad (1)$$

We drop the subscript e for electrons wherever this will cause no confusion. AI are equivalent to setting $h_i = 0$, so that $g_i = -e\langle\phi\rangle F/T$ only, taking ion and electron temperatures equal. The quasineutrality equation then becomes simply $2e\phi n/T = -\int d^3\mathbf{v}\langle h\rangle_\mathbf{r}$. The integral is the perturbed electron density at particle coordinate $\mathbf{r}$.

We use the Abel-Barnes model collision operator [6], including electron-ion collisions. There is no drag offset term because $h_i = 0 \Rightarrow u_{\parallel i} = 0$ (the parallel ion flow; cf. equation (35) of Ref. [6]). In $\mathbf{k}_\perp$ space:

$$\langle C[h_{\mathbf{k}_\perp}]\rangle = C_{\mathrm{GK}}^{ee}[h_{\mathbf{k}_\perp}] + \nu_D^{ei}\left[\frac{1}{2}\frac{\partial}{\partial\xi}(1-\xi^2)\frac{\partial h_{\mathbf{k}_\perp}}{\partial\xi} - \frac{1}{4}(1+\xi^2)\frac{v^2}{v_{te}^2}k_\perp^2\rho_e^2 h_{\mathbf{k}_\perp}\right]. \qquad (2)$$

The two terms in the bracket are respectively the electron-ion pitch-angle scattering, and finite-Larmor-radius (FLR) diffusion. Analogous terms are present in the electron-electron piece of the model operator, C_{GK}^{ee}, which also includes correction terms so that it conserves particle number, momentum and energy. Electron-ion collisions relax the parallel electron flow; that is, resistively dissipate the parallel current. As a result, the electron-ion piece of the operator, and hence the operator overall, does not conserve (electron) momentum. Electron-electron collisions conserve momentum locally in real space, but in gyrocentre space the electron-electron FLR diffusion introduces dissipation for all modes except $k_\perp = 0$. However, the FLR diffusion terms are small by a factor $k_\perp^2\rho_e^2$, so the dominant momentum-non-conservation overall comes from pitch-angle scattering in the electron-ion piece of the operator.

In our simulations below, we use a flux-tube geometry with nominal parameters specified in Table I. The flux-tube domain has $-\pi \le \theta \le \pi$, where θ is the poloidal angle coordinate. ($\theta = 0$ is the outboard midplane, $\theta = \pm\pi$ the inboard midplane.) The spatial grid has $N_\theta = 48$ cells in the parallel direction, and 80×108 points in the perpendicular $x \times y$ directions, in which the cross-section is square with minimum and maximum positive k_y of $1.4/\rho_i$ and $49/\rho_i \approx 0.8/\rho_e$ respectively. There are $N_\mathcal{E} = 18$ energy grid points, and $N_p = 16$ pitch-angles for passing particles in each direction. There is one pitch-angle for trapped particles bouncing at each θ grid point. Note that, because of the twist-and-shift parallel boundary conditions in flux-tube geometry [7, 8], some of the lower nonzero k_y's have longer linked domains than the single 2π range of θ. $h = 0$ for the incoming direction at both ends of the linked domain. Periodic boundary conditions are applied in the perpendicular direction.

minor radius	r/a	0.65
major radius	R/a	1.46
safety factor	q	1.9
magnetic shear	$\hat{s}$	1.8
Shafranov shift	Δ/a	−0.25
elongation	κ	1.57
	κ'	0.40
triangularity	δ	0.22
	δ'	0.16
fprim	a/L_n	−1.2
tprim	a/L_T	3.42
collisionality	$\nu_{\mathrm{nom}}a/v_{ti}$	1.39

TABLE I. Nominal local equilibrium parameters (based approximately on MAST shot 8500 at $t = 0.289\,\mathrm{s}$). $a = 0.55\,\mathrm{m}$ is the minor radius of the LCFS, the macroscopic normalizing length. The heat flux Q will be normalized by $Q_{GB} = n_i T_i v_{ti}(\rho_{ti}/a)^2$, where ρ_{ti} is the thermal ion gyroradius, the microscopic normalizing length. In electron units $\nu_{\mathrm{nom}} = 0.02\,v_{te}/a$.

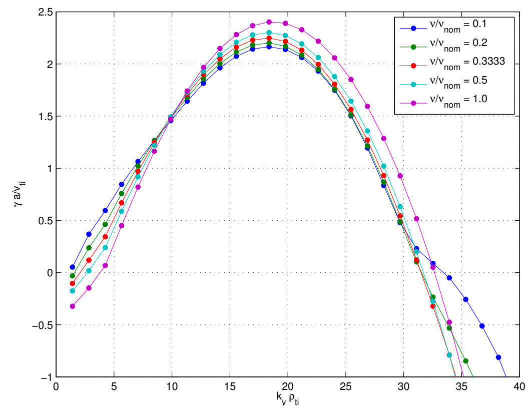

FIG. 1. Linear growth rates versus k_y, at $k_x = 0$ (with zero flow shear), for several collisionalities.

A small amount of flow shear, $\gamma_E = -0.188\,v_{ti}/a$, was included in the nonlinear simulations; as in Ref. [4], this was found to assist convergence and is of the same order as the experimental level in MAST.

Figure 1 shows the maximum linear growth rate at each k_y in the numerical domain. These linear simulations have zero flow shear, and the growth rate at $k_x = 0$ is given. At low k_y, the growth rate increases as collisionality is decreased, narrowing the stable region; the lowest $k_y > 0$ is unstable at the lowest collisionality shown here. At high k_y, the growth rate decreases with collisionality. Except at the lowest and highest k_y's – and especially at the mid-range k_y's which dominate the nonlinearly saturated heat flux – the fractional change in growth rate is small compared to the order-of-magnitude change in collisionality. We conjecture that these modest changes in the linear spectrum are not the cause of large changes in nonlinear saturation over the same range of collisionality.

HEAT FLUX SCALING WITH COLLISIONALITY

Figure 2 shows the variation of the time-averaged heat flux with collisionality and temperature gradient. The reduction in heat flux with collisionality can clearly be seen.

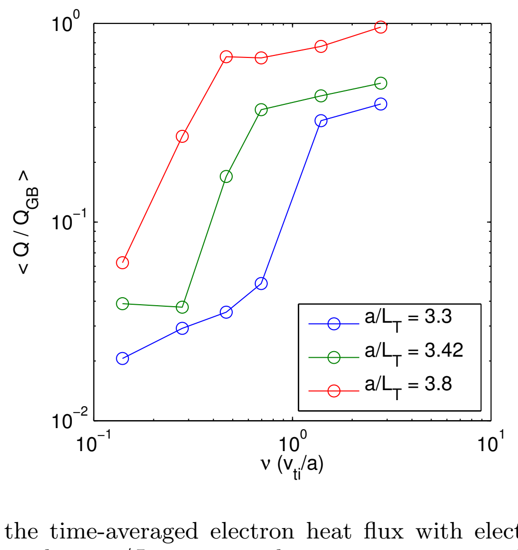

FIG. 2. Variation of the time-averaged electron heat flux with electron collisionality, at the nominal temperature gradient, $a/L_T = 3.3$, and one temperature gradient on either side.

ZONAL FLOWS

Figure 3 shows the heat flux and the zonal potential squared versus time for points on the blue curve in Figure 2, $a/L_T = 3.3$. After the initial linear growth phase, the heat flux 'quasi-saturates' nonlinearly. However, the zonal potential continues to grow slowly, leading to an eventual fall in the heat flux (starting at $t \sim 50\,a/v_{ti}$). Prior to this time, the evolution is statistically indistinguishable for the different collisionalities. However, the final saturated level after the fall is a function of collisionality (as shown in Figure 2). The onset time and the rate of fall are also functions of collisionality, but converge as the collisionality is reduced: the lowest three collisionalities in Figure 3 overlay each other.

* Permanent address: Department of Nuclear and Quantum Engineering, KAIST, Daejeon, Korea.

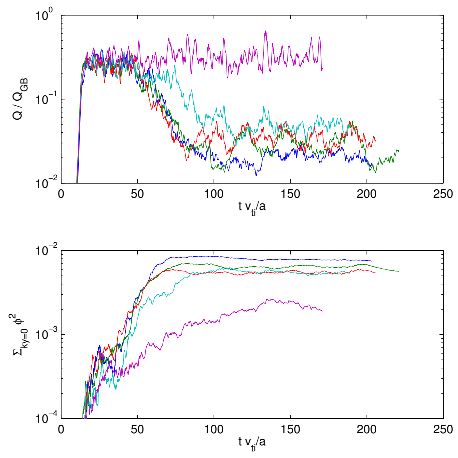

FIG. 3. Evolution of the turbulent electron heat flux (top) and the square of the zonal potential (bottom) as a function of time, for $a/L_T = 3.3$ and various collisionalities (colors as Figure 1).

We obtain some insight into the mechanism for the damping of the zonal potential by looking at the linear damping rates of the zonal modes, in simulations restarted from the nonlinear saturated state but with the nonlinearity ($\langle \mathbf{v}_E \rangle \cdot \nabla h$ in equation (1)) now turned off. Figure 4 shows that the zonal damping rate $\nu_Z \propto \nu k_x^2$, a scaling indicative of spatial diffusion. As mentioned above, the FLR diffusion terms in the gyrokinetic collision operator are small. These terms correspond to the displacement of gyrocentres by distances $\sim \rho_e$ due to collisions during Larmor rotation. However, considered on the longer transit timescale, collisions also cause the displacement of banana (and corresponding passing) orbits by distances $\sim \rho_{pe}$, which is larger. Indeed, we find that if we turn off magnetic drifts ($\mathbf{v}_d \cdot \nabla h$ in equation (1)), the zonal damping rates drop by approaching an order of magnitude, as shown by the blue open circles in Figure 4. The figure also shows that the dominant contribution to the damping is from electron-ion collisions; when these are turned off (black crosses), the damping rates drop by more than an order of magnitude in the $k_x \rho_{ti} \leq 10$ range of interest. This evidence is all consistent with zonal damping $\nu_Z \sim \nu_{ei} k_x^2 \rho_{pe}^2$, arising physically from electron-ion collisions that do not conserve parallel (electron) momentum and produce spatial diffusion on the banana-width scale.

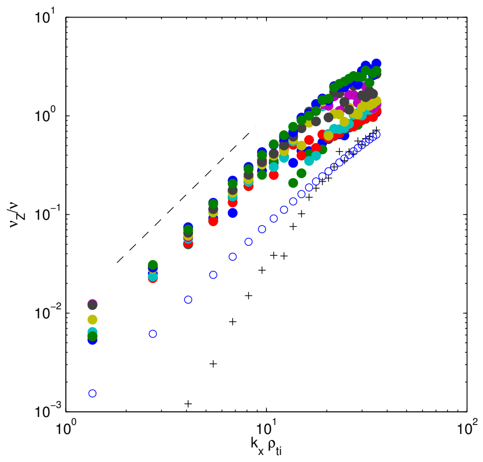

FIG. 4. Zonal damping rate over collisionality, ν_Z/ν, versus k_x, for various collisionalities (solid colors). The dashed line is $\propto k_x^2$. Also shown are the corresponding rates for a run in which electron-ion collisions were turned off (black crosses); and a run in which electron-ion collisions were retained but magnetic drifts were turned off (blue open circles).

EXPLAINING THE VARIATION OF HEAT FLUX WITH COLLISIONALITY

In the GKE for a typical nonzonal mode, if we assume that the nonlinear term is dominated by nonzonal-zonal interactions, and that in the saturated state these balance the drive term $\langle \mathbf{v}_E \rangle \cdot \nabla F$, then we obtain

$$k_x h_{\mathrm{Z}} \sim F/L. \tag{3}$$

(This is a form of mixing-length hypothesis, that the perturbed gradients ∇h flatten the background gradient ∇F.)

In the GKE for a typical zonal mode, there are only nonzonal-nonzonal interactions, and no linear drive (since ∇F is in the x direction). In this case, we can balance the nonlinear term against collisional damping, giving

$$k_x k_y \phi_{\mathrm{NZ}} h_{\mathrm{NZ}}/B \sim \nu_{\mathrm{Z}} h_{\mathrm{Z}}. \tag{4}$$

We use subscripts Z, NZ to denote zonal and nonzonal respectively. Taking $h_{\mathrm{Z}}/\phi_{\mathrm{Z}} \sim h_{\mathrm{NZ}}/\phi_{\mathrm{NZ}} \sim eF/T$ and combining equations (3) and (4) we get

$$\left(\frac{h_{\mathrm{NZ}}}{h_{\mathrm{Z}}}\right)^2 \sim \left(\frac{\phi_{\mathrm{NZ}}}{\phi_{\mathrm{Z}}}\right)^2 \sim \frac{\nu_{\mathrm{Z}} eBL}{k_y T}, \tag{5}$$

$$\frac{Q}{Q_{\mathrm{GB}}} \sim k_y \rho_t \left(\frac{e\phi_{\mathrm{NZ}}}{T(\rho_t/R)}\right)^2 \sim \frac{\nu_{ei}}{(v_t/R)} \frac{R}{L} \left(\frac{\rho_p}{\rho_t}\right)^2. \tag{6}$$

Alternatively, if the nonlinear term acts as a source at high frequency $\omega \gg \nu_{\mathrm{Z}}$, then equation (4) will be replaced by a scaling

$$k_x k_y \phi_{\mathrm{NZ}} h_{\mathrm{NZ}}/B \sim \sqrt{\omega \nu_{\mathrm{Z}}} h_{\mathrm{Z}}, \tag{7}$$

and the explicit scaling of the heat flux with collisionality will be $Q \propto \sqrt{\nu_{ei}}$ instead.

RELATIONSHIP TO EARLIER WORK

At large enough R/L_T or ν_{ei}, the zonal flow does not rise to a level high enough to produce the long-time fall in heat flux, which therefore remains at its 'quasi-saturated' – in that case truly saturated – level. This can be seen at the highest collisionality in Figure 3, and is also evident in the lack of collisionality dependence at the high-collisionality end of Figure 2. In the high-R/L_T limit we may recover the 'critical balance' scaling obtained for ion-temperature-gradient (ITG) turbulence by Barnes et al. [9] (which did not involve collisionality).

The effect of zonal damping on the saturated level of turbulence has previously been considered for ITG [10], and by Kim et al. for ETG [11]; in the large-aspect-ratio limit, they found that (as for the ITG case [12, 13]) the zonal damping time is shorter than the electron collision time. At the aspect ratio of order unity considered in the present paper, we find that the nonlinear state evolves on a time scale longer than the collision time.

Long-time changes in the saturated state of gyrokinetic simulations have been seen by others [14–16]. Some previous ETG results may be only 'quasi-saturated', but further exploration in parameter space is necessary to determine the full scope of these effects.

Microtearing has also been suggested as a possible explanation for the experimental transport scaling in STs [17, 18]. Whilst microtearing is an inherently electromagnetic effect and cannot explain electrostatic results, we note that the theoretical arguments in the present paper do not depend explicitly on the nature of the instabilities driving the turbulence. We leave a more detailed consideration of this issue to further work.

CONCLUSIONS

In summary, we find that ETG turbulence simulations at driving gradients close to experimental levels and at low collisionality must be run to long times to capture the effect of zonal flows on the saturated state, and at these long times we find that heat transport Q_e decreases with collisionality ν_e. This is favorable towards improved confinement in future (hotter, hence less collisional) devices such as CTF [19]. We have explained this behavior theoretically by balancing nonlinear and drive or damping terms in the GKE for nonzonal and zonal modes.

ACKNOWLEDGMENTS

This work was part-funded by the RCUK Energy Programme under grant EP/I501045, and by the European Union's Horizon 2020 research and innovation programme under grant agreement number 633053. Computations were performed at the UK's HECToR service under EPSRC grant EP/H002081/1, on EFDA's HPC-FF system, and on Helios at IFERC-CSC.

The authors thank Greg Hammett, Walter Guttenfelder, Ian Abel, Steve Cowley, Edmund Highcock and Ferdinand van Wyk for enlightening discussions; and thank Anthony Field, Martin Valovič, Martin O'Brien and Francis Casson for helpful comments on drafts of this paper.

[1] S. M. Kaye, F. M. Levinton, D. Stutman, K. Tritz, H. Yuh, M. G. Bell, R. E. Bell, C. W. Domier, D. Gates, W. Horton, J. Kim, B. P. LeBlanc, N. C. Luhmann Jr, R. Maingi, E. Mazzucato, J. E. Menard, D. Mikkelsen, D. Mueller, H. Park, G. Rewoldt, S. A. Sabbagh, D. R. Smith, and W. Wang, Nuclear Fusion **47**, 499 (2007).

[2] M. Valovič, R. Akers, M. de Bock, J. McCone, L. Garzotti, C. Michael, G. Naylor, A. Patel, C. Roach, R. Scannell, M. Turnyanskiy, M. Wisse, W. Guttenfelder, J. Candy, and the MAST team, Nuclear Fusion **51**, 073045 (2011).

[3] A. R. Field, C. Michael, R. J. Akers, J. Candy, G. Colyer, W. Guttenfelder, Y. C. Kim, C. M. Roach, S. Saarelma, and the MAST team, in *Proceedings of 23rd IAEA Fusion Energy Conference, Daejon, Republic of Korea, EXC/P8-04* (2010).

[4] C. M. Roach, I. G. Abel, R. J. Akers, W. Arter, M. Barnes, Y. Camenen, F. J. Casson, G. Colyer, J. W. Connor, S. C. Cowley, D. Dickinson, W. Dorland, A. R. Field, W. Guttenfelder, G. W. Hammett, R. J. Hastie, E. Highcock, N. F. Loureiro, A. G. Peeters, M. Reshko, S. Saarelma, A. A. Schekochihin, M. Valovic, and H. R. Wilson, Plasma Physics and Controlled Fusion **51**, 124020 (2009).

[5] GS2 is an open-source code hosted at http://gyrokinetics.sourceforge.net/.

[6] I. G. Abel, M. Barnes, S. C. Cowley, W. Dorland, and A. A. Schekochihin, Physics of Plasmas **15**, 122509 (2008).

[7] M. Beer, *Gyrofluid models of turbulent transport in tokamaks*, Ph.D. thesis, University of Princeton (1995).

[8] M. A. Beer, S. C. Cowley, and G. W. Hammett, Physics of Plasmas **2**, 2687 (1995).

[9] M. Barnes, F. I. Parra, and A. A. Schekochihin, Phys. Rev. Lett. **107**, 115003 (2011).

[10] Z. Lin, T. S. Hahm, W. W. Lee, W. M. Tang, and P. H. Diamond, Phys. Rev. Lett. **83**, 3645 (1999).

[11] E.-j. Kim, C. Holland, and P. H. Diamond, Phys. Rev. Lett. **91**, 075003 (2003).

[12] F. L. Hinton and M. N. Rosenbluth, Plasma Physics and Controlled Fusion **41**, A653 (1999).

[13] Y. Xiao, P. J. Catto, and K. Molvig, Physics of Plasmas **14**, 032302 (2007).

[14] W. Guttenfelder and J. Candy, Physics of Plasmas **18**, 022506 (2011).

[15] M. Nakata, T.-H. Watanabe, H. Sugama, and W. Horton, Physics of Plasmas **17**, 042306 (2010).

[16] P. Mantica, C. Angioni, B. Baiocchi, M. Baruzzo, M. N. A. Beurskens, J. P. S. Bizarro, R. V. Budny, P. Buratti, A. Casati, C. Challis, J. Citrin, G. Colyer, F. Crisanti, A. C. A. Figueiredo, L. Frassinetti, C. Giroud, N. Hawkes, J. Hobirk, E. Joffrin, T. Johnson, E. Lerche, P. Migliano, V. Naulin, A. G. Peeters, G. Rewoldt, F. Ryter, A. Salmi, R. Sartori, C. Sozzi, G. Staebler, D. Strintzi, T. Tala, M. Tsalas, D. V. Eester, T. Versloot, P. C. deVries, J. Weiland, and JET EFDA Contributors, Plasma Physics and Controlled Fusion **53**, 124033 (2011).

[17] W. Guttenfelder, J. Candy, S. M. Kaye, W. M. Nevins, R. E. Bell, G. W. Hammett, B. P. LeBlanc, and H. Yuh, Physics of Plasmas **19**, 022506 (2012).

[18] W. Guttenfelder, J. Peterson, J. Candy, S. Kaye, Y. Ren, R. Bell, G. Hammett, B. LeBlanc, D. Mikkelsen, W. Nevins, and H. Yuh, Nuclear Fusion **53**, 093022 (2013).

[19] G. Voss, S. Davis, A. Dnestrovskij, A. Kirk, P. Knight, M. Loughlin, M. O'Brien, D. Sychugov, A. Tabasso, and H. Wilson, Fusion Engineering and Design **83**, 1648 (2008).